Registry No. $[Ni(H_2O)_2(dl\text{-chxn})_2]Cl_2$, 53748-64-4; $[Ni(H_2O)_2(dl\text{-chxn})_2]Br_2$, 65859-01-0; $[Ni(H_2O)_2(dl\text{-chxn})_2](NO_3)_2$, 53748-66-6; $[Ni(H_2O)_2(dl\text{-chxn})_2](ClO_4)_2$, 65835-90-7; $[NiCl_2(dl\text{-chxn})_2]$, 110454-60-9; $[NiBr_2(dl\text{-chxn})_2]$, 110417-89-5; $[Ni(NO_3)_2(dl\text{-chxn})_2]$, 110392-11-5; $[Ni(dl\text{-chxn})_2]Cl_2$, 53748-60-0; $[Ni(dl\text{-chxn})_2]Br_2$, 53748-61-1; $[Ni(dl\text{-chxn})_2](ClO_4)_2$, 53748-63-3; $[Ni(NO_3)(ms\text{-chxn})_2](NO_3)$, 110392-13-7; $[Ni(ms\text{-chxn})_2](NO_3)_2$, 110454-56-3; $[Ni(ms\text{-chxn})_2]Cl_2$, 110454-57-4; $[Ni(ms\text{-chxn})_2]Br_2$, 110454-58-5; $[Ni(ms\text{-chxn})_2](ClO_4)_2$, 110454-59-6.

Supplementary Material Available: Listings of analytical data (SM Table I) and electronic spectral data and magnetic moments of the prepared complexes (SM Table II) (2 pages). Ordering information is given on any current masthead page.

Contribution from the Departments of Chemistry, Washington State University, Pullman, Washington 99164-4630, and Leiden University, 2300 RA Leiden, The Netherlands

Crystal Structures and Magnetic Behavior of Pyridinium Bis(oxalato)cuprate(II)–Oxalic Acid and Bis(2-methylimidazole)copper(II) Oxalate

U. Geiser,[1a] B. L. Ramakrishna,[1a] R. D. Willett,*[1a] F. B. Hulsbergen,[1b] and J. Reedijk[1b]

Received April 1, 1987

The crystal structure and magnetic properties of two oxalato complexes of copper(II) are reported. Pyridinium bis(oxalato)-cuprate(II)–oxalic acid (triclinic, $P\bar{1}$, a = 8.980 (6) Å, b = 14.159 (7) Å, c = 3.697 (3) Å, α = 92.47 (7)°, β = 101.17 (7)°, γ = 97.69 (4)°, R = 0.039) contains stacks of $Cu(ox)_2^{2-}$ anions with long semicoordinate bonds between copper(II) ions in one anion to a coordinated oxygen atom in each adjacent anion in the stack. Magnetic susceptibility data reveal weak antiferromagnetic coupling (Θ = −3.6 K from Curie–Weiss law behavior). Analysis of the EPR spectrum sets a lower limit of $|J| \sim 10^{-2}$ cm^{-1} for the intrachain coupling. Bis(2-methylimidazole)(oxalato)copper(II) (orthorhombic, $Pbc2_1$, a = 8.235 (2) Å, b = 19.565 (5) Å, c = 7.994 (2) Å, R = 0.049) contains a distorted square pyramidally coordinated copper(II) ion. The equatorial plane contains two nitrogen atoms (one each from an imidazole ligand) and two oxygen atoms from a chelated oxalato ligand. The apical site is occupied by an uncoordinated oxygen atom from an oxalato group on an adjacent complex. This forms a chain structure parallel to the c axis. The magnetic susceptibility data indicate weak ferromagnetic coupling for this compound with J/k = 0.45 (4) K. Analysis of the EPR line width data yields an estimate of $|J| \sim 0.1$ cm^{-1}.

Introduction

Magnetostructural correlations (i.e., the change of magnetic interaction with slight variations in the bridging geometry) have been demonstrated in copper(II) and chromium(III) compounds with ligands bridging through one atom between the metal centers.[2] It has been known for a long time that magnetic exchange can take place through more complex bridging networks, the most famous compound probably being the classical dimer $(H_2O)Cu(CH_3CO_2)_4Cu(H_2O)$.[3] More recently, the polyatomic anions azide, N_3^-, and oxalate, $C_2O_4^{2-}$, have been shown to form magnetically coupled dimers and chains with copper(II).[4,5]

Kahn[5] demonstrated that the strongest antiferromagnetic interaction occurs when the bridging oxalate ion is coplanar with the copper $d_{x^2-y^2}$ magnetic orbitals, assuming an essentially tetragonal ligand field geometry (see Figure 1a). On the other hand, very little exchange is observed when one oxalate oxygen atom coordinates to an apical site (Figure 1b). Asymmetric bridging with one copper of each of these types leads to intermediate coupling.

The role of oxalate as a bridging ligand is not confined to dimeric systems. The strongly antiferromagnetically coupled compound $CuC_2O_4 \cdot {}^1/_3H_2O$ is believed to consist of ribbons with the bridge framework as shown in Figure 1a.[6] Several salts of the bis(oxalato)cuprate(II) anion have been investigated in a search of strong magnetic interaction, preferably of low-dimensional nature. Benzylammonium copper oxalate forms layers of $Cu(C_2O_4)_2^{2-}$ ions connected by long (2.6 Å) bonds between an outer oxygen atom and an adjacent copper ion at the axial position. The magnetic interaction for such a bridging arrangement is very small, J/k = −0.2 K.[7] Propylenediammonium copper oxalate forms stacks of bis(oxalato)cuprate(II) anions (vide infra). The coupling is very weak, and obscured in the noise of the susceptibility data.[7] Other bis(oxalato)cuprate(II) salts with known crystal structures include the sodium,[8] ammonium, potassium,[9] and 1,3-diammonium-2-propanol salts.[10] The first three of these all show weak antiferromagnetic coupling.[7,8,11] The aim of this paper is to present two new linear-chain copper oxalate compounds, pyridinium bis(oxalato)cuprate(II)–oxalic acid (PCOX) and bis(2-methyl-imidazole)(oxalato)copper(II) (MICO) with their synthesis, crystal structures, magnetic susceptibilities, and electron paramagnetic resonance spectra. The planar nature of the counterions and ligands were expected to induce different crystal packing and, hopefully, as a consequence, different magnetic properties.

Experimental Section

Synthesis. Copper(II) oxalate hydrate was prepared by reacting green copper(II) carbonate ($CuCO_3 \cdot Cu(OH)_2$) with a slight excess of oxalic acid hydrate in warm aqueous suspension. After the mixture was stirred for 2 h, gas evolution ceased and the suspended solid was light blue. Filtering proved to be very difficult. Instead, the suspension was allowed to stand, and most of the supernatant could be drawn off after several hours. Meanwhile, a stoichiometric amount of pyridine was carefully neutralized with oxalic acid in water. This solution was added to the copper(II) oxalate slurry, which in turn became darker blue. Pyridine

(1) (a) Washington State University. (b) Leiden University.
(2) Hatfield, W. E. In *Magneto-Structural Correlations in Exchange Coupled Systems*; Willett, R. D., Gatteschi, D., Kahn, O., Eds.; NATO ASI Series, Series C 140u; Reidel: Dordrecht, The Netherlands, 1985; p 555. Hodgson, D. J. *Ibid.*; p 497.
(3) Bleaney, B.; Bowers, K. D. *Proc. R. Soc. London, A* **1952**, *214*, 451.
(4) Hendrickson, D. In *Magneto-Structural Correlations in Exchange Coupled Systems*; NATO ASI Series, Series C 140u; Reidel: Dordrecht, The Netherlands, 1985; p 523.
(5) Girerd, J. J.; Kahn, O.; Verdaguer, M. *Inorg. Chem.* **1980**, *19*, 274. Julve, M.; Verdaguer, M.; Kahn, O.; Gleizes, A.; Philoche-Levisalles, M. *Inorg. Chem.* **1983**, *22*, 368. Julve, M.; Verdaguer, M.; Charlot, M.-F.; Kahn, O.; Claude, R. *Inorg. Chem. Acta* **1984**, *82*, 5.
(6) Michalowicz, A.; Girerd, J. J.; Goulon, J. *Inorg. Chem.* **1979**, *18*, 3004.
(7) Bloomquist, D. R.; Hansen, J. J.; Landee, C. P.; Willett, R. D.; Buder, R. *Inorg. Chem.* **1981**, *20*, 3308. Mennenga, G.; Bartolome, J.; deJongh, L. J.; Willett, R. D. *Chem. Phys. Lett.* **1984**, *105*, 351.
(8) Gleizes, A.; Maury, F.; Galy, J. *Inorg. Chem.* **1980**, *19*, 2074.
(9) Viswamitra, M. A. *J. Chem. Phys.* **1962**, *37*, 1408. Viswamitra, M. A. *Z. Kristallogr., Kristallgeom., Kristallphys., Kristallchem.* **1962**, *117*, 437.
(10) Kivekäs, R.; Pajunen, A. *Cryst. Struct. Comm.* **1977**, *6*, 477.
(11) Jeter, D. Y.; Hatfield, W. E. *Inorg. Chim. Acta* **1972**, *6*, 523.

0020-1669/87/1326-3750$01.50/0

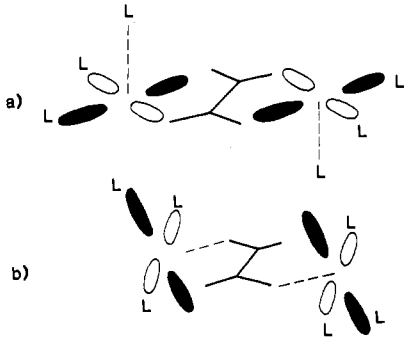

Figure 1. Schematic view of the Cu^{2+}–oxalate dimer, showing two orientations of the copper $d_{x^2-y^2}$ orbitals: (a) coplanar with the oxalate ion; (b) perpendicular to the oxalate ion. L = N or O donor.

Table I. Crystal Data and Data Collection[a]

	PCOX	MICO
space group	$P\bar{1}$	$Pbc2_1$
a, Å	8.980 (6)	8.235 (2)
b, Å	14.159 (7)	19.565 (5)
c, Å	3.697 (3)	7.994 (2)
α, deg	92.47 (7)	
β, deg	101.17 (7)	
γ, deg	97.69 (4)	
V, Å^3	455.91	1288.07
Z	1	4
d_{calcd}, g/cm^3	1.78	1.63
no. of rflcns collcd	3324 ($h,k,l \leq 0$)	2112 ($h \geq 0, k \geq 0, l \geq 0$)
no. of unique, nonextinct reflcns	3228	2007
no. of reflcns with $F > 2\sigma$	3132	1746
μ, cm^{-1}	13.4	17.4
transmissn factors	0.67–0.76	0.70–0.84
2θ(max) (λ = 0.710 69 Å), deg	65	60
std reflcns[b]	600, 4$\bar{5}$0, 0$\bar{8}$0	340, 270, 241

[a] PCOX = pyridinium bis(oxalato)cuprate(II)–oxalic acid. MICO = bis(2-methylimidazole)(oxalato)copper(II). [b] Measured after every 41 reflections.

was added until all of the copper(II) oxalate dissolved, yielding a bright blue solution. Blue flat, elongated crystals of pyridinium bis(oxalato)cuprate(II)–oxalic acid formed after slow evaporation. The frequently occurring laminar twins are readily recognized under the polarizing microscope. Anal. Found (calcd): Cu, 13.15 (12.97); C, 39.48 (39.23); N, 5.62% (5.78); H, 2.54 (2.88).

The bis(2-methylimidazole) compound was formed by slow evaporation of an aqueous solution containing a stoichiometric ratio of $Cu(CH_3CO_2)_2 \cdot H_2O$ and 2-methylimidazole and a twofold excess of $Na_2C_2O_4$. This produced dark blue prisms, typically capped on one side with rooflike end faces. Anal. Found (calcd): C, 37.66 (38.04); N, 17.69 (17.74); H, 4.03 (3.83).

X-ray Work. The crystal structures were determined at room temperature (293 ± 2 K). Preliminary results were obtained by Weissenberg and precession film techniques. The data collection was carried out on a Picker automated four-circle diffractometer, controlled by the Oak Ridge program package.[12] The orientation matrix and lattice parameters were optimized from the least-squares refinement to the angular settings of 12 carefully centered reflections with high Bragg angles. These results and details of the data collection are given in Table I. Data collection was carried out with θ–2θ scans and a peak width of 2°. Zr-filtered Mo Kα radiation (λ = 0.710 69 Å) was used. Sets of atomic parameters are given in Tables II and III.

The data reduction included adjustment to the least-squares linear decay curve obtained from the intensities of three standard reflections (measured after every 41 peaks), absorption corrections, Lorentz and polarization factors, and cross-scaling of two or three sets with different attenuation filters. The standard deviations of the intensities were estimated as $\sigma^2(I) = TC + BC + (0.03I)^2$, where TC = total count, BC = background count, and I = TC–BC. The calculations were carried out on Washington State University's Amdahl 470/V8 computer under VM/CMS using a program package described elsewhere.[13a] Scattering factor tables from standard sources for Cu^{2+}, O, N, C[14a], and H[14b] were used. The scattering factors were corrected for anomalous dispersion effects.

Table II. Fractional Coordinates and Equivalent Anisotropic Thermal Parameters in Pyridinium Bis(oxalato)cuprate(II)–Oxalic Acid

atom	x	y	z	U,[a] Å^2
Cu	0.00000	0.00000	0.00000	0.030
O(1)	−0.0234 (1)	0.13461 (7)	−0.0023 (3)	0.032
O(2)	−0.1700 (1)	−0.01377 (7)	0.2459 (4)	0.040
O(3)	−0.1797 (1)	0.23039 (7)	0.1672 (3)	0.038
O(4)	−0.3420 (1)	0.07125 (8)	0.3937 (4)	0.042
O(5)	−0.0020 (1)	0.37685 (8)	−0.0066 (4)	0.043
O(6)	−0.1654 (1)	0.46588 (8)	0.1707 (4)	0.044
N	0.5258 (2)	0.2254 (1)	0.5025 (4)	0.035
C(1)	−0.1379 (2)	0.15135 (9)	0.1322 (4)	0.025
C(2)	−0.2282 (2)	0.06358 (9)	0.2669 (4)	0.029
C(3)	−0.0524 (2)	0.45700 (9)	0.0524 (4)	0.028
C(4)	0.5715 (2)	0.3187 (1)	0.5595 (5)	0.038
C(5)	0.4720 (3)	0.3760 (1)	0.6612 (5)	0.043
C(6)	0.3270 (3)	0.3355 (2)	0.6947 (5)	0.051
C(7)	0.2852 (2)	0.2381 (2)	0.6351 (5)	0.046
C(8)	0.3888 (2)	0.1836 (1)	0.5390 (5)	0.040

[a] U is one-third of the trace of the orthogonalized U_{ij} tensor.

Table III. Fractional Coordinates and Equivalent Anisotropic Thermal Parameters in Bis(2-methylimidazole)copper(II) Oxalate

atom	x	y	z	U,[a] Å^2
Cu	0.21890 (6)	0.15741 (2)	0.25000	0.025
O(1)	0.4082 (4)	0.1212 (2)	0.1243 (5)	0.030
O(2)	0.2194 (4)	0.2260 (2)	0.0713 (5)	0.036
O(3)	0.3906 (4)	0.2698 (2)	−0.1160 (5)	0.037
O(4)	0.5859 (4)	0.1566 (2)	−0.0662 (6)	0.042
N(11)	−0.0137 (5)	0.1726 (2)	0.3021 (5)	0.029
N(12)	−0.2565 (5)	0.2147 (3)	0.3414 (7)	0.038
N(21)	0.2482 (5)	0.0814 (2)	0.4117 (6)	0.030
N(22)	0.3109 (6)	−0.0198 (2)	0.5048 (8)	0.048
C(1)	0.4600 (6)	0.1629 (2)	0.0147 (7)	0.028
C(2)	0.3495 (6)	0.2255 (2)	−0.0135 (7)	0.028
C(11)	−0.1016 (6)	0.2295 (2)	0.3037 (6)	0.032
C(12)	−0.1209 (6)	0.1200 (3)	0.3410 (9)	0.039
C(13)	−0.2693 (7)	0.1455 (3)	0.3638 (9)	0.042
C(14)	−0.0445 (7)	0.3005 (3)	0.274 (1)	0.048
C(21)	0.2555 (7)	0.0154 (3)	0.3754 (8)	0.039
C(22)	0.3016 (7)	0.0876 (3)	0.5743 (8)	0.040
C(23)	0.3404 (9)	0.0246 (4)	0.630 (1)	0.056
C(24)	0.2091 (9)	−0.0155 (3)	0.2129 (9)	0.057

[a] U is one-third of the trace of the orthogonalized U_{ij} tensor.

Magnetic Measurements. Electron paramagnetic resonance spectra were measured on a Varian E-3 X-band spectrometer. The powdered samples were placed in 4-mm-diameter quartz tubes while single crystals were oriented by X-ray diffraction techniques and mounted on a goniometer capable of rotation around a single axis. A small quartz Dewar filled with liquid N_2 was used for the low-temperature (77 K) experiments.

The magnetic susceptibilities were measured on a Princeton Applied Research (PAR) Model 155 vibrating sample magnetometer. A PAR 152 unit was used to control the temperature via a heater feedback circuit controlled by a GaAs diode. Cryogenic temperatures were achieved with a Janis 153 flow cryostat suitable for work with either liquid helium or liquid nitrogen. A conventional electromagnet was employed to produce magnetic fields of up to 10 kOe (1 T). Temperature was measured by using either a thermocouple (liquid-nitrogen region) or a germanium resistance thermometer (liquid-helium region) calibrated as previously described.[13b]

(12) Busing, W. R.; Ellison, R. D.; Levy, H. A.; King, S. P., Roseberry, R. T. Report ORNL-4135; Oak Ridge National Laboratory; Oak Ridge, TN, 1968.

(13) (a) Geiser, U.; Willett, R. D.; Gaura, R. M. *Acta Crystallogr., Sect. C: Cryst. Struct. Commun.* **1984**, *C40*, 1346. (b) Geiser, U.; Gaura, R. M.; Willett, R. D.; West, D. *Inorg. Chem.* **1986**, *25*, 4203.

(14) (a) *International Tables for X-Ray Crystallography*; Kynoch: Birmingham, England, 1962; Vol. III. (b) Stewart, R. F.; Davidson, E. R. and Simpson, W. T. *J. Chem. Phys.* **1965**, *42*, 3175.

Table IV. Interatomic Distances (Å) and Angles (deg) in Pyridinium Bis(oxalato)cuprate(II)–Oxalic Acid[a]

distances		angles	
	Copper Coordination Sphere		
Cu–O(1)	1.945 (1)	O(1)–Cu–O(2)	85.61 (6)
Cu–O(2)	1.915 (2)	O(1)–Cu–O(2^{i})	94.79 (7)
Cu–O(2^{i})[b]	2.893 (3)	O(2)–Cu–O(2^{i})	81.51 (8)
	Ligand Oxalate		
C(1)–O(1)	1.270 (2)	Cu–O(1)–C(1)	111.6 (1)
C(2)–O(2)	1.281 (2)	Cu–O(2)–C(2)	112.5 (1)
C(1)–O(3)	1.237 (2)	O(1)–C(1)–O(3)	125.8 (1)
C(2)–O(4)	1.220 (2)	O(2)–C(2)–O(4)	124.6 (1)
C(1)–C(2)	1.546 (2)	O(1)–C(1)–C(2)	115.3 (1)
		O(2)–C(2)–C(1)	114.6 (1)
		O(3)–C(1)–C(2)	118.8 (1)
		O(4)–C(2)–C(1)	120.8 (1)
	Oxalic Acid		
C(3)–O(5)	1.302 (2)	O(5)–C(3)–C(3^{ii})	111.4 (2)
C(3)–O(6)	1.200 (2)	O(6)–C(3)–C(3^{ii})	122.6 (2)
C(3)–C(3)	1.547 (3)	O(5)–C(3)–O(6)	126.0 (1)
O(5)–H(O)	0.90 (4)	C(3)–O(5)–H(O)	108 (2)
	Pyridinium Cation		
N–C(4)	1.325 (2)	C(8)–N–C(4)	123.6 (2)
C(4)–C(5)	1.377 (3)	N–C(4)–C(5)	118.7 (2)
C(5)–C(6)	1.381 (3)	C(4)–C(5)–C(6)	119.6 (2)
C(6)–C(7)	1.377 (3)	C(5)–C(6)–C(7)	119.6 (2)
C(7)–C(8)	1.373 (3)	C(6)–C(7)–C(8)	118.8 (2)
C(8)–N	1.325 (2)	C(7)–C(8)–N	119.7 (2)
N–H(N)	0.85 (4)		
C(5–8)–H(C(5–8))	0.8–1.0		
	Hydrogen Bonding		
H(O)···O(3)	1.72 (4)	C(1)–O(3)···H(O)	118 (1)
O(3)···O(5)	2.624 (2)	O(3)···H(O)–O(5)	174 (3)
H(N^{iii})···O(4)	1.86 (4)	C(2)–O(4)···H(N^{iii})	124 (1)
O(4)···N	2.672 (2)	O(4)···H(N^{iii})–N^{iii}	160 (3)

[a] Esd's are given in parentheses. [b] Key: (i) $-x, -y, 1-z$; (ii) $-x, 1-y, -z$; (iii) $-1+x, y, z$.

Solution and Description of the Structures

Pyridinium Bis(oxalato)cuprate(II)–Oxalic Acid. The intensity distribution and chemical intuition both indicated the centrosymmetric space group $P\bar{1}$. This choice was confirmed by the successful refinement. Copper and the coordinated oxygen atoms were located on a Patterson synthesis. Direct methods gave the same result and further peaks on an *E*-map were identified as additional oxygen, nitrogen, and carbon atoms. The remaining non-hydrogen atoms were found from a difference Fourier synthesis. Full-matrix least-squares refinement (based on *F*) was carried out by using $1/\sigma^2$ weights. Only reflections with $F > 2\sigma$ were included in the refinement. Two scale factors, positional parameters (except Cu), and anisotropic thermal parameters were varied. Hydrogen atoms were then located and their positions refined. Agreement factors were[15] $R = 0.039$, $R_w = 0.043$ with 164 varied parameters. The final difference electron density map was featureless, with extrema of −0.4 and 0.3 e/Å^3.

Relevant interatomic distances and angles of PCOX are given in Table IV. The bis(oxalato)cuprate(II) complex ion is located at a center of inversion at the origin. The two oxalate ions coordinate in the usual planar chelating fashion. O(2) deviates most from a least-squares planar through the complex (0.085 (1) Å), being slightly displaced toward the next copper ion of the chain, to which it is semicoordinated. The coordination sphere of the copper ion is best described as 4 + 2. The chelating oxygens are at the normal distance of 1.93 Å in the average, whereas the distance to the semicoordinated O(2) atoms is 2.89 Å. The compound thus forms uniform stacks of bis(oxalato) cuprate ions along the crystallographic *c*- axis as seen in Figure 2. O(2) is the bridging atom between two adjacent copper ions (Cu···Cu = 3.697 Å apart). A similar structure type was also found in

(15) $R = \sum(||F_o| - |F_c||)/\sum|F_o|$. $R_w = \sum(w(|F_o| - |F_c|)^2/\sum|F_o|^2)^{1/2}$.

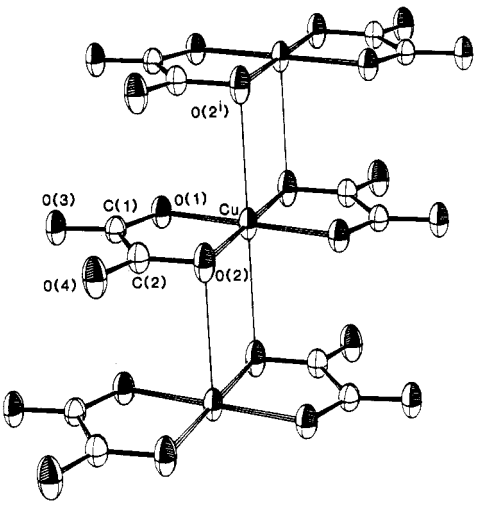

Figure 2. Chain structure in pyridinium bis(oxalato)cuprate(II)–oxalic acid.

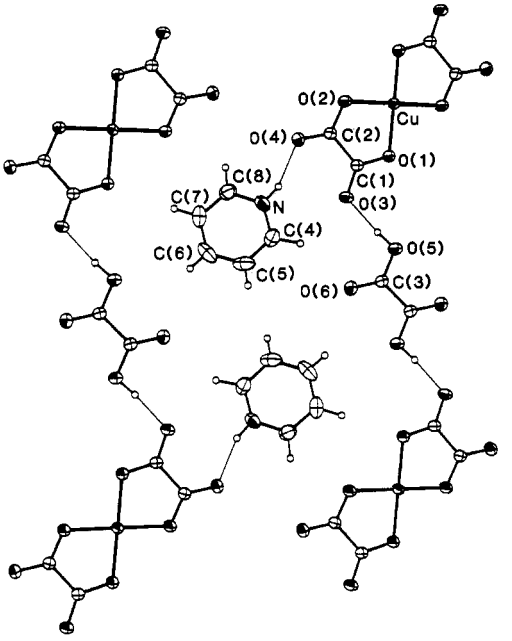

Figure 3. Cross section through the structure of pyridinium bis(oxalato)cuprate(II)–oxalic acid perpendicular to the chain axis. Hydrogen bonds are indicated by thin lines. The *b* axis is vertical.

$Na_2Cu(C_2O_4)_2 \cdot 2H_2O$,[7] but in the present compound the chains are far more isolated magnetically.

Along the *b* axis, these chains are connected by hydrogen-bond linkages involving the lattice oxalic acid molecule, as illustrated in Figure 3. A somewhat similar arrangement of both coordinated and neutral ligands occurs in the oxamide oxime complex[16] of copper(II) with stoichiometry $[Cu(C_2H_5N_4O_2)_2] \cdot C_2H_6N_4O_2$. The hydrogen atom of the oxalic acid molecule is clearly resolved, and the carbon–oxygen distances are different for the two inequivalent oxygens, the one carrying the hydrogen being noticeably longer (1.30 Å) than the other (1.20 Å). The O···O contact of 2.62 Å is indicative of a relatively strong hydrogen bond. The least-squares plane through the oxalic acid molecule forms a dihedral angle of only 6.0° to the plane of the bis(oxalato) cuprate(II) complex, and the atom O(3), to which the hydrogen bond points, as well as the hydrogen atom itself, is within 0.002 Å of the plane. The cleavage plane $(10\bar{2})$ contains the chain axis and these hydrogen-bonding linkages.

The space in the center of the unit cell is occupied by the two symmetry-related pyridinium cations. The acidic H(N) is hy-

(16) Endres, H.; Genc, N.; Nöthe, D. *Acta Crystallogr., Sect. C: Cryst. Struct. Commun.* **1983**, *C39*, 701.

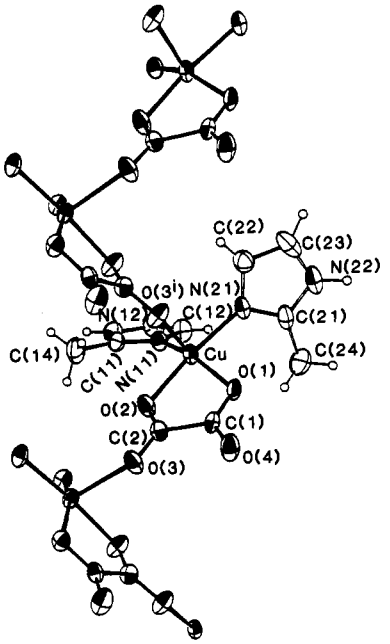

Figure 4. Chain structure of bis(2-methylimidazole)(oxalato)copper(II). The ligands are completely drawn in only one complex for clarity. The view is approximately along the *a* axis.

drogen bound to one of the terminal oxygens of the ligand oxalate (N···O of 2.67 Å). Relatively large thermal parameters within the plane of the cation indicate the possibility of some librational disorder. The pyridinium ion is planar with an average deviation of 0.005 Å from a least-squares plane; the sum of the internal angles is 719.98° (instead of 720°). The plane forms a dihedral angle of 21° to the plane through the bis(oxalato)copper ion, and O(4), which participates in the hydrogen bond to the pyridinium cation, is 0.294 (1) Å away from the plane. The ring is distorted from an ideal hexagon in that the carbon–nitrogen distances are ca. 0.05 Å shorter than the carbon–carbon bonds, and the angle at the nitrogen atom (123.6°) is by far the largest in the ring.

Bis(2-methylimidazole)(oxalato)copper(II). A Patterson synthesis and direct methods (both centrosymmetric and noncentrosymmetric) indicated the copper atom, but no other clear-cut results emerged at this stage. The positions of the other atoms were sought from electron density difference maps. The peaks obtained from the mirror symmetry of the space group *Pbcm* did not make chemical sense, and therefore, it was decided to continue on in the noncentrosymmetric space group $Pbc2_1$ (a nonstandard setting of $Pca2_1$). The structure refined successfully with the latter choice. The space group is polar, and the *z* position of Cu was held fixed at 0.25. Since the structure factors calculated from the copper atom alone are real, another atom, O(2), had to be included in the starting set in order to bias the difference synthesis. All non-hydrogen atoms were located on subsequent cycles. In the full-matrix least-squares refinement of the structure, all positional (except *z* of Cu) and anisotropic thermal parameters were refined. Hydrogen atoms were then located on a difference map, and the positional parameters of the non-methyl hydrogens were included in the refinement. Two reflections (200 and 021) were assigned zero weight because of secondary extinction. Otherwise all reflections with $F > 2\sigma$ were included in the refinement with weights of $1/\sigma^2$. The final agreement factors were $R = 0.049$ and $R_w = 0.043$. A total of 191 parameters were varied. No attempt was made to determine the correct handedness of the structure.

Bond distances and angles are given in Table V. The structure (Figure 4) consists of essentially isolated chains along the *z* axis. The chains contain the *c*-glide plane perpendicular to *b*. The two independent neutral 2-methylimidazole molecules act as monodentate ligands in a cis orientation whereas the oxalate ion forms a chelating ring with the copper on one side. The coordination sphere is completed by a distinctly longer bond to one of the terminal oxygen atoms of an adjacent oxalate (Cu···O = 2.276 Å). The coordination geometry at the copper center can be described as intermediate between square pyramidal and trigonal bipyramidal with a long equatorial bond. The intermediate nature is illustrated by the dihedral angles between adjacent faces of the coordination polyhedron (Table VI; cf. ref 17a). This distortion

Table V. Interatomic Distances (Å) and Angles (deg) in Bis(2-methylimidazole)(oxalato)copper(II)[a]

distances		angles	
	Copper Coordination Sphere		
Cu–O(1)	1.985 (3)	O(1)–Cu–O(2)	82.7 (1)
Cu–O(2)	1.961 (4)	O(1)–Cu–N(11)	156.7 (2)
Cu–N(11)	1.983 (4)	O(1)–Cu–N(21)	88.1 (2)
Cu–N(21)	1.985 (4)	O(1)–Cu–O(3ⁱ)	88.5 (1)
Cu–O(3ⁱ)[b]	2.276 (4)	O(2)–Cu–N(11)	93.0 (2)
		O(2)–Cu–N(21)	170.8 (2)
		O(2)–Cu–O(3ⁱ)	85.0 (2)
		N(11)–Cu–N(21)	95.3 (2)
		N(11)–Cu–O(3ⁱ)	114.1 (2)
		N(21)–Cu–O(3ⁱ)	95.0 (2)
	Ligand Oxalate		
C(1)–O(1)	1.270 (6)	Cu–O(1)–C(1)	112.6 (3)
C(2)–O(2)	1.268 (6)	Cu–O(2)–C(2)	112.7 (3)
C(1)–O(4)	1.223 (6)	O(1)–C(1)–O(4)	125.7 (4)
C(2)–O(3)	1.239 (6)	O(2)–C(2)–O(3)	125.4 (4)
C(1)–C(2)	1.543 (7)	O(1)–C(1)–C(2)	114.3 (4)
		O(2)–C(2)–C(1)	115.3 (4)
		O(3)–C(2)–C(1)	119.4 (4)
		O(4)–C(1)–C(2)	120.0 (4)
		C(2ⁱ)–O(3ⁱ)–Cu	125.4 (3)
	2-Methylimidazole Ligands		
N(11)–C(11)	1.329 (6)	C(12)–N(11)–C(11)	105.8 (4)
C(11)–N(12)	1.343 (7)	N(11)–C(11)–N(12)	109.8 (4)
N(12)–C(13)	1.371 (8)	C(11)–N(12)–C(13)	108.4 (4)
C(13)–C(12)	1.333 (8)	N(12)–C(13)–C(12)	106.4 (5)
C(12)–N(11)	1.391 (7)	C(13)–C(12)–N(11)	109.6 (5)
C(11)–C(14)	1.485 (7)	N(11)–C(11)–C(14)	127.6 (4)
N(12)–H(N12)	0.88 (10)	N(12)–C(11)–C(14)	122.6 (4)
C(12)–H(C12)	0.77 (9)	Cu–N(11)–C(11)	130.8 (3)
C(13)–H(C13)	1.07 (9)	Cu–N(11)–C(12)	123.3 (3)
N(21)–C(21)	1.326 (7)	C(22)–N(21)–C(21)	106.1 (5)
C(21)–N(22)	1.324 (8)	N(21)–C(21)–N(22)	110.5 (6)
N(22)–C(23)	1.349 (10)	C(21)–N(22)–C(23)	108.0 (5)
C(23)–C(22)	1.350 (9)	N(22)–C(23)–C(22)	107.3 (7)
C(22)–N(21)	1.377 (8)	C(23)–C(22)–N(21)	108.0 (6)
C(21)–C(24)	1.482 (9)	N(21)–C(21)–C(24)	125.3 (5)
N(22)–H(N22)	0.96 (9)	N(22)–C(21)–C(24)	124.2 (5)
C(22)–H(C22)	0.91 (10)	Cu–N(21)–C(21)	126.4 (4)
C(23)–H(C23)	0.93 (11)	Cu–N(21)–C(22)	126.0 (4)

[a] Esd's are given in parentheses. [b] Key: (i) $x, {}^1/_2 - y, {}^1/_2 + z$.

Table VI. Dihedral Angles (deg) between Normals to the Adjacent Faces of the Coordination Polyhedron in Bis(2-methylimidazole)(oxalato)copper(II) (MICO) and Idealized Bodies[a]

	TBP	EBP	MICO	ESP	SQP
δa_1	101.5	99.0	104.3	119.4	119.8
δa_3	101.5	99.0	115.1	119.4	119.8
δa_4	101.5	99.0	108.5	119.4	119.8
δa_6	101.5	99.0	120.1	119.4	119.8
δa_2	101.5	102.7	83.6	76.0	75.7
δa_5	101.5	102.7	84.1	76.0	75.7
δe_1	53.1	56.2	70.8	76.0	75.7
δe_2	53.1	56.2	66.4	76.0	75.7
δe_3	53.1	53.1	20.8	0.0	0.0

[a] The notation is from Muetterties and Guggenberger.[17a] TBP = trigonal bipyramid with equal center–ligand distances. EBP = triangular bipyramid with an elongated equatorial ligand (long/short = 1.15 as in MICO). SQP = square pyramid with equal center–ligand distances and an eq–c–ax angle of 102°. ESP = axially elongated (1.15) square pyramid using 95.64° (average angle in MICO). In order to remain consistent with the notation of ref 17a the axial ligands are A_1 = O(2) and A_2 = N(21), whereas the equatorial ligands are E_1 = O(1), E_2 = O(3′), and E_3 = N(11) (bipyramid limit).

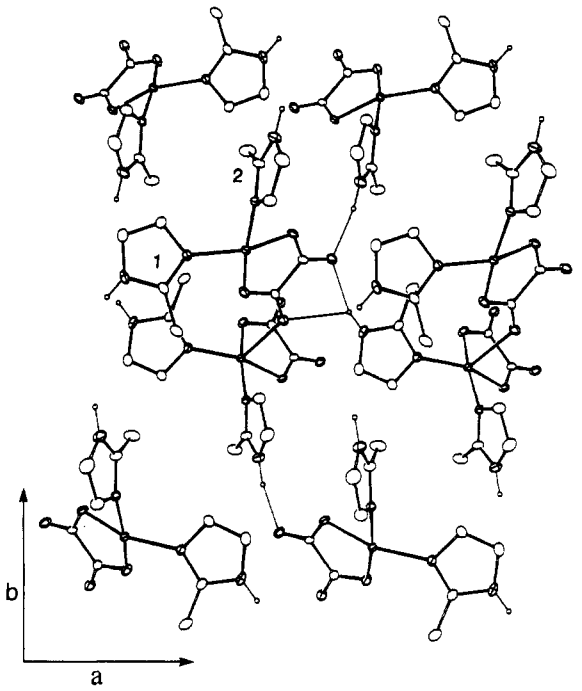

Figure 5. Crystal packing of bis(2-methylimidazole)(oxalato)copper(II). Hydrogen bonds between methylimidazoles and neighboring oxalates are indicated by thin lines. Ring numbers are referred to in the text.

has been more simply characterized by Addison et al.[17b] by a parameter, $\tau = (\theta_1 - \theta_2)/60$, where θ_1 and θ_2 are the two trans angles in the basal plane ($\tau = 0$ for square pyramidal; $\tau = 1$ for trigonal bipyramidal). For this compound, $\tau = 0.24$. In light of the large O(1)–Cu–N(11) angle (156.7°), the coordination is best described as square pyramidal with a superimposed C_{2v} distortion. The orientation between adjacent members of the chain can be characterized in different ways. The angle between neighboring Cu–O(3) bonds (i.e. the local z axis in the distorted square-pyramidal model) is 77.5 (2)°, whereas the angle between the least-squares planes through the basal ligand atoms O(1), O(2), N(11), and N(21) is 80.4°. Alternatively, the angle between planes formed by O(1), Cu, and O(2) is 70.3 (3)°. The shortest copper–copper distance, across the oxalate ion, is 5.395 (1) Å. This is caused by the distortion toward trigonal-bipyramidal geometry.

The methylimidazole ligands are essentially planar. In ring 1 (indicated by atomic numbers 11–14) all atoms are within 0.004 Å from the least-squares plane, the sum of the internal angles is 539.99°, and the methyl carbon atom is 0.026 (9) Å out of the plane. At the same time the copper ion is 0.0596 (1) Å from the plane, on the opposite side. The deviations from the least-squares plane in ring 2 are even smaller, maximum 0.002 Å, and the angles add to 539.99°. The methyl carbon atom is almost exactly in the plane, but the copper ion is 0.3826 (5) Å away.

Adjacent chains are connected through N···O hydrogen bonds, as shown in Figure 5. The hydrogen atom on N(12) forms a slightly asymmetric, bifurcated bond to the outer oxalate oxygens of a chain related by a unit cell translation along the a axis. The hydrogen on N(22) joins with O(4) located on a chain related by a screw translation along the c axis.

Magnetic Susceptibility

Both pyridinium bis(oxalato)cuprate(II)–oxalic acid and bis(2-methylimidazole)copper(II) oxalate have susceptibilities closely following Curie's law (Figures 6 and 7). The solid curve in Figure 6 was obtained from the Curie-Weiss formula $\chi = C/(T - \Theta)$ with $C = 0.4077$ (9) and $\Theta = -3.6$ (14) K for the pyridinium compound. For $C = Ng^2\beta^2S(S + 1)/(3k)$, this yields $g = 2.085$ with $S = {}^1/_2$,

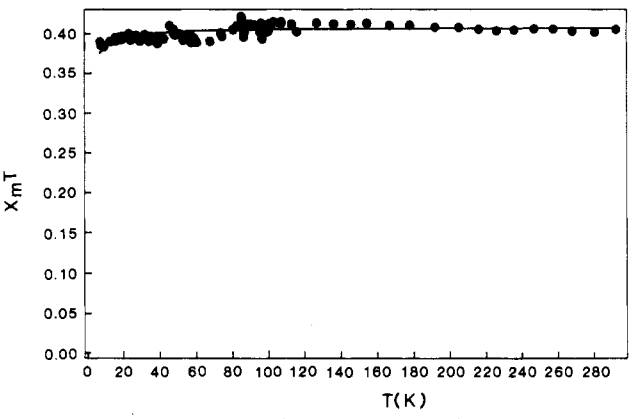

Figure 6. Product of molar powder susceptibility and temperature versus T for pyridinium bis(oxalato)cuprate(II)–oxalic acid: (●) observed values; (—) curve calculated from Curie–Weiss law by using $g = 2.085$ and $\Theta = -3.6$.

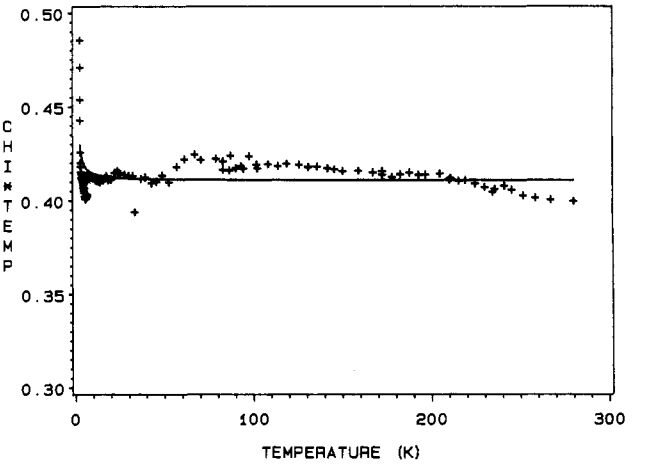

Figure 7. Product of molar powder susceptibility and temperature versus T for bis(2-methylimidazole)(oxalato)copper(II): (+) observed values; (—) curve calculated by using $J/k = 0.45$ K and $g = 2.099$.

in accordance with EPR spectra. The methylimidazole compound, of which several data sets are drawn in Figure 7, shows an increasing moment at very low temperatures. The fitted curve is that of a ferromagnetic Heisenberg $S = {}^1/_2$ chain[18] with $J/k = 0.45$ (4) K and $g = 2.099$ (7). At the high-temperature end the moments drop somewhat below the calculated curve, probably due to systematic errors in the measurement. The data sets show considerable scatter at low temperature, but all show the onset of a rapid increase of $\chi_M T$ (and thus of the moment) below about 5 K.

EPR

Theory. From magnetic susceptibility data it is clear that the exchange interaction in these compounds is weak. However, measurements to much lower temperatures would be needed in order to evaluate a reliable value of J. In the weak-exchange regime where $J/k < 1$ K, EPR is a sensitive probe and has the advantage that one does not have to go down to very low temperatures to obtain the relevant information.

It has been shown[19] that in crystals with magnetically equivalent sites, the angular dependence of the exchange-narrowed EPR line provides a simple and direct method for evaluating high-temperature Fourier components of the spin-correlation function. As the general theory of magnetic resonance in exchange-coupled systems has been dealt with in detail by Kubo and Tomita,[20] we shall only briefly review the method used.

(17) (a) Muetterties, E. L.; Guggenberger, L. J. *J. Am. Chem. Soc.* **1974**, *96*, 1748. (b) Addison, A. W.; Rao, T. N.; Reedijk, J.; van Rijn, J.; Verschoor, G. C. *J. Chem. Soc., Dalton Trans.* **1984**, 1349.

(18) Baker, G. A., Jr.; Rushbrooke, G. S.; Gilbert, H. E. *Phys. Rev.* **1964**, *135*, A1272.

(19) Soos, Z. G.; McGregor, K. T.; Cheung, T. T. P.; Silverstein, A. J. *Phys. Rev.* **1977**, *B16*, 3036.

(20) Kubo, R.; Tomita, K. *J. Phys. Soc. Jpn.* **1954**, *9*, 888.

Soos starts with a zeroth-order Hamiltonian

$$\mathcal{H}_0 = \mathcal{H}_{zee} + \mathcal{H}_{ex} \quad (1)$$

Local dipolar and hyperfine fields are treated as a perturbation to $\mathcal{H}_0$ and lead to small deviations $\Delta\omega$ from ω_0, the Larmor resonance frequency, with $\Delta\omega \ll \omega_0$. The modulation of these local fields by the exchange interaction leads to the local field correlation function

$$\Psi(\tau) = \langle \Delta\omega(\tau)\, \Delta\omega(0) \rangle \quad (2)$$

and is related to the relaxation function, $\phi(t)$, by

$$\phi(t) = \exp\left[-\int_0^t (t-\tau)\, \Psi(\tau)\, d\tau\right] \quad (3)$$

The resonance absorption is given by the frequency Fourier transform of $\phi(t)$. The above equation can be simplified, when $\hbar/J \ll$ relaxation time characterizing $\phi(t)$ (i.e., J in frequency units much larger than the deviations $\Delta\omega$ caused by local fields) to

$$\phi(t) = \exp\left[-t\int_0^\infty \Psi(\tau)\, d\tau\right] \quad (4)$$

The peak-to-peak derivative line width, ΔH_{pp}, is then given by

$$\Delta H_{pp} = \int_0^\infty \Psi(\tau)\, d\tau \quad (5)$$

$\Psi(\tau)$ is the basic quantity of interest for theoretically predicting the line width. The magnitude of its time independent part, $\Psi(0)$, is given by the second moment of local fields, and the time dependence can be evaluated by assuming a particular form for the spin-correlation function, which is governed by the exchange parameter.

The local field correlation $\Psi(\tau)$ contains both dipolar and hyperfine contributions, each of which can be separated into secular and nonsecular forms. Each individual contribution can be obtained by multiplying the corresponding time-independent second moment with a Fourier component coming from the time dependence.

The total line width Γ ($=(3^{1/2}/2)\Delta H_{pp}$) is given by

$$\Gamma_{total} = \Gamma_{hyp} + \Gamma_{dip} \qquad \Gamma_{hyp} = a^{(0)}\, g(0) + a^{(1)}\, g(\omega)$$
$$\Gamma_{dip} = M_2^{(0)}\, f(0) + M_2^{(1)}\, f(\omega) + M_2^{(2)}\, f(2\omega) \quad (6)$$

where $a^{(0)}$ and $a^{(1)}$ are the secular and nonsecular hyperfine second moments and $M_2^{(0)}$, $M_2^{(1)}$, and $M_2^{(2)}$ are the secular and the two nonsecular dipolar second moments. The expressions for evaluating these are straightforward and are taken from the paper by Soos et al.[19] The Fourier components of an autocorrelation function, $C(t)$, yield the two-spin hyperfine correlation functions $g(0)$ and $g(\omega)$ whereas the Fourier components of $C^2(t)$ give the four-spin dipolar correlation functions $f(0)$, $f(\omega)$, and $f(2\omega)$.

The angular and frequency dependence of the EPR line width thus provide enough equations to solve for the unknowns: $g(0)$, $g(\omega)$, $f(0)$, $f(\omega)$, and $f(2\omega)$. All that remains is to relate these experimentally determined Fourier components to the exchange parameter by assuming a theoretical model for the autocorrelation function $C(t)$.

Results. The line width analysis shall be carried out in detail only for the pyridinium compound for two reasons. First, an approximate estimate of the exchange parameter (1000 G) showed that in this case it is much greater than the contributions from the broadening mechanisms, whereas for the methylimidazole compound (150 G) it is found to be little more than the dipolar and hyperfine terms. The theory has not been well developed for the latter case of very weak exchange, and the approximations made above are clearly not valid. Secondly, the structure of PCOX is triclinic with one molecule per unit cell; hence, we expect only one magnetically distinct site in the crystal. The analysis of the line width variation for that case is fairly straightforward as one does not have to contend against the effects of g averaging on line width as in the case of MICO. However, we shall first briefly discuss the results for MICO, and it will be clear that it is at least possible to estimate some limits for the value of the exchange constant.

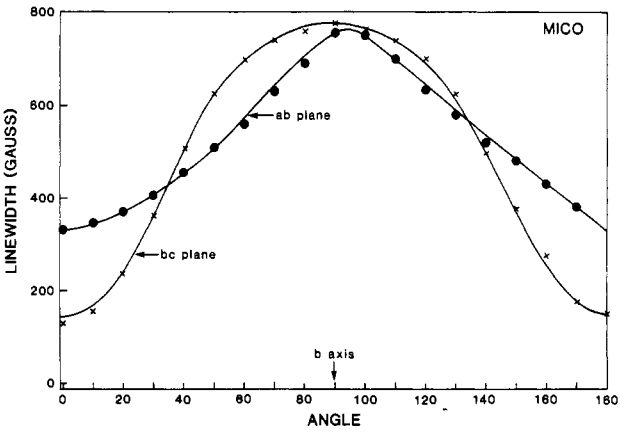

Figure 8. EPR line width in *ab* (●) and *bc* (×) planes for bis(2-methylimidazole)(oxalato)copper(II). Solid line is only a guide to the eyes.

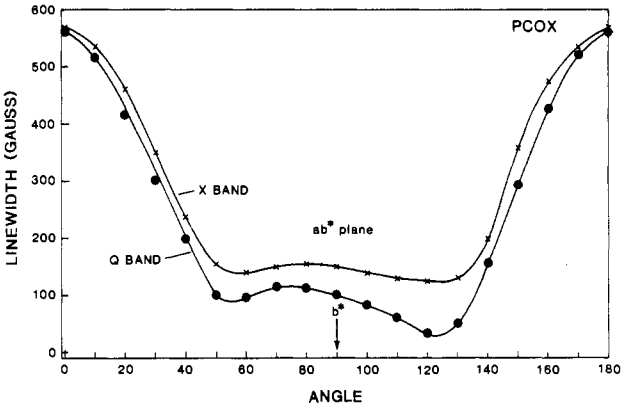

Figure 9. EPR line width in the *ab** plane for pyridinium bis(oxalato)-cuprate(II)–oxalic acid at X-band (×) and Q-band (●). Solid line is only a guide to the eyes.

In MICO, the CuN_2O_2 entity is nearly planar and hence one can assume that $g_\parallel$ is perpendicular to that plane. The direction cosines for $g_\parallel$ of two neighboring copper units within the reference chain (1) with respect to a, b, and c are 0.435, 0.645, and 0.628 and 0.435, −0.645, and 0.628. Similarly for the rotated set of chains, they are −0.435, −0.645, and 0.628 and −0.435, 0.645, and 0.628. The EPR spectra in the *ab* and *bc* planes consist of a single line with the line width varying from about 100 G to nearly 800 G (Figure 8). From the space group symmetry this observation can be explained if the exchange coupling within a chain (along the c axis) is larger than the g anisotropy. In this case, $g_\parallel$ is perpendicular to the chain direction, and from the observed geometry, the cosines of the resultant $g_\parallel$ direction with the crystal axes can be deduced for the two chain orientations in the crystal as 0.569, 0, and 0.822 and −0.569, 0, and 0.822. This allows the extraction of the g anisotropy ($\sim$100 G) and, therefore, a lower limit for the intrachain exchange coupling as $\sim 10^{-2}$ cm^{-1}. In addition, the fact that in the *ac* plane two resonances are observed at many orientations allows us to estimate an upper limit for interchain exchange of $\sim$80 G.

To obtain a more complete picture of the nature and strength of the various magnetic interactions in PCOX, measurements were made at both X- and Q-band frequencies. Only the nonsecular second moments contribute to the differences in line width observed at X- and Q-band frequencies, with the X-band line width predicted to be always larger than the Q-band width (Figures 9 and 10). A nonlinear least-squares fit of this difference yields the differences in the nonsecular Fourier components at X- and Q-bands. With the help of this information one can fit the angular dependence of line width at either frequency in any given plane to obtain the five unknowns of eq 6. The values obtained from

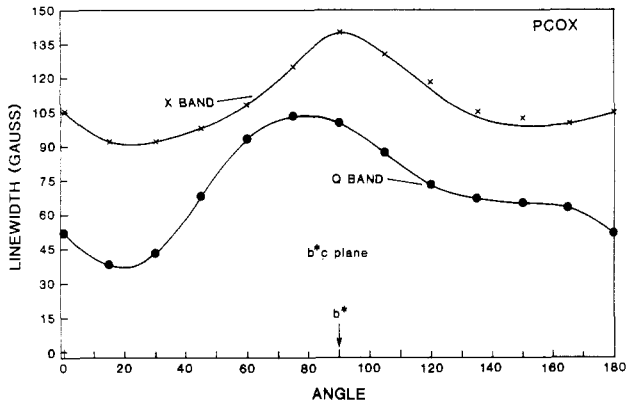

Figure 10. EPR line width in the b^*c plane for pyridinium bis(oxalato)cuprate(II)–oxalic acid at X-band (×) and Q-band (●). Solid line is only a guide to the eyes.

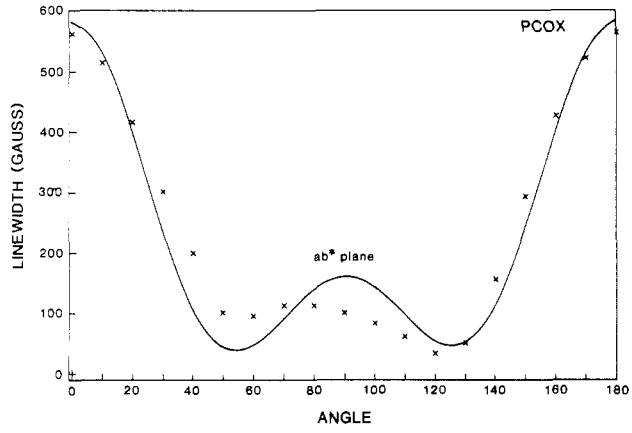

Figure 11. Theoretical fit of Q-band EPR line widths for pyridinium bis(oxalato)cuprate(II)–oxalic acid.

the fitting of the Q-band line width in the *ab* plane (Figure 11) are $f(0) = 1.06 \times 10^{-3}$ G^{-1}, $f(\omega) = 1 \times 10^{-4}$ G^{-1}, $f(2\omega) = 1 \times 10^{-5}$ G^{-1}, $g(0) = 1.5 \times 10^{-3}$ G^{-1} and, $g(\omega) = 1 \times 10^{-3}$ G^{-1}. Assuming the Blume–Hubbard model for the autocorrelation function $C(t)$

$$C_{BH}(t) = \cosh^{-2}(\tfrac{1}{2}\hat{J}t) \tag{7}$$

the Fourier components for the dipolar and hyperfine terms are calculated as

$$f_{BH}(x) = \tfrac{1}{2}\int_{-\infty}^{\infty}[\exp(i\omega t)]\, C^2(t)\, dt = (4/3\hat{J})(x/(\sinh x))[1 + (x/\pi)^2]$$

$$g_{BH}(x) = \tfrac{1}{2}\int_{-\infty}^{\infty}[\exp(i\omega t)]\, C(t)\, dt = (2/\hat{J})(x/(\sinh x)) \tag{8}$$

where $x = \pi\omega/\hat{J}$ is a scaled frequency and $\hat{J}$ is the root-mean-square pairwise exchange at a given site. The limit as $x \to 0$ gives the secular Fourier components

$$f(0) = 4/3\hat{J} \qquad g(0) = 2/\hat{J} \tag{9}$$

From the experimentally determined values of $f(0)$ and $g(0)$ (see above), values for $\hat{J}$ of 1258 and 1333 G, respectively, are obtained. As the crystal structure reveals that the copper units form a chain with each site coupled to two neighbors (one on each side along the chain) the exchange between two sites is obtained to be $\hat{J}/2^{1/2}$, or 920 G $\simeq$ 0.1 cm^{-1}.

Discussion

At first glance it might be surprising that these two compounds show very little, if any, magnetic interaction. This is particularly true for the pyridinium salt, where the copper–copper distance is only 3.7 Å. In contrast, an antiferromagnetic exchange of several hundred Kelvin has been found in some oxalate species with distances up to 5.4 Å between copper centers. In those compounds, however, the oxalate ion served as a doubly chelating bridge, and the additional ligands were arranged in such a manner that the $d_{x^2-y^2}$ orbitals, which contain the unpaired electron, lie in the plane of the oxalate ion. Dimers are known where the addition of a strong donor in the ligand position perpendicular to that plane, on one or both of the copper atoms, causes the reversal of the magnetic orbitals with an associated decrease of the absolute value of the interaction. These results confirm the general validity of Kahn's arguments concerning the importance of this orbital reversal in determining magnetic exchange coupling.

In the pyridinium compound the magnetic orbital lies in the $Cu(ox)_2^{2-}$ plane, while the superexchange pathway involves interactions between adjacent planes. All orbitals that could possibly be involved in superexchange pathway are confined to the oxalate plane (the $d_{x^2-y^2}$ orbital does not mix with any of the ligand π orbitals), and the overlap density between σ-type orbitals is expected to be rather small across a gap of 2.9 Å (perpendicular distance between adjacent bis(oxalato)cuprate units). The appearance of small antiferromagnetic coupling reflected in the negative Weiss constant cannot be explained because any of the conceivable, though inefficient, exchange pathways involve orthogonal orbitals and thereby suggest a slightly ferromagnetic interaction. The observed very weak antiferromagnetism may be associated with dipolar coupling mechanisms, either of an intra- or interchain type.

In the methylimidazole compound the copper atom is surrounded by five ligands in a rather irregular geometry. This makes the assignment of a magnetic orbital rather difficult. If we assume a coordination derived from square pyramidal, with atom $O(3')$ at the apex, a $d_{x^2-y^2}$-type orbital is a reasonable approximation. Such an orbital lies in the plane of the chelating oxalate ion to form an extended magnetic orbital. If this assignment is correct, there is negligible delocalization from the neighboring copper center onto the bridging O(3) atom of the oxalate, virtually eliminating a large superexchange interaction. In addition, the magnetic orbital of the neighbor is in a spatial arrangement that makes any remaining overlap approximately orthogonal and therefore causes a ferromagnetic interaction. This is indeed observed, with an exchange constant of less than 1 K. The fit of the susceptibility measurements to the theoretical prediction of the one-dimensional Heisenberg model (Figure 11) is rather poor, however.

Acknowledgment. The support of NSF Grant DMR-8219430 and of a ZWO grant (The Netherlands) is gratefully acknowledged. The award of a Fulbright-Hayes Fellowship to R.D.W. is strongly appreciated.

Registry No. PCOX, 110142-31-9; MICO, 110142-33-1.

Supplementary Material Available: Listings of anisotropic thermal parameters and hydrogen atom positions (3 pages); tables of observed and calculated structure factors (23 pages). Ordering information is given on any current masthead page.